

Redbourn, L.J., Bull, J.M., Scrutton, R.A., Stow, D.A.V.S. 1993. Channels, echo character mapping and tectonics from 3.5 kHz profiles, distal Bengal Fan. *Marine Geology*, **114**: 155-170

Channels, Echo Character Mapping and Tectonics from 3.5kHz Profiles, Distal Bengal Fan.

Lisa J. Redbourn¹, Jonathan M. Bull^{1,3}, Roger A. Scrutton² and Dorrik A.V. Stow¹

1 Department of Geology, University of Southampton, Highfield, Southampton SO9 5NH

2 Department of Geology and Geophysics, University of Edinburgh, West Mains Road, Edinburgh EH9 3JW

3 Author to whom correspondence should be addressed.

ABSTRACT

The distal parts of the Bengal Fan are spectacularly affected by tectonic deformation related to the diffuse plate boundary between the Indian and Australian plates. Here we use 3.5kHz and 12kHz echosounder profiles, seismic reflection profiles and piston core results to examine sedimentary processes and their relationships to tectonism within an area (78°-82°E, 0°-6°S) just to the south of Ocean Drilling Program Leg 116 sites.

Echo character mapping was completed using echosounder data in conjunction with results from piston coring, and a total of five different echo types have been recognised. Four of these fall into the echo character classification scheme developed by Damuth (1980a), whilst the fifth is believed to represent hemiturbidite deposits. Several types of submarine channel were also identified from echosounder data and a correlation between echo type and channel location can be seen. Their abundance, erosional and/or depositional nature together with a complex meandering and bifurcation pattern across a wide region of average gradient around 1°/km, are all features characteristic of a broad channel termination zone on a large elongate fan. It is clear,

therefore that the Bengal Fan extends beyond 6°S.

Active faulting in the area has led to the development of an irregular topography of low rounded hillocks that interfere with incoming turbidity currents. This has resulted in ponding between highs rather than lobe construction, thinning and pinching out of turbidites against the flanks of local relief, flow lofting and hemiturbidite drape, and common small-scale slumping. In some cases uplifted channel segments can be seen abandoned and partially filled.

INTRODUCTION

The Bengal Fan (Fig. 1) is one of the world's largest elongate submarine fans and has an area of $2.8\text{--}3 \times 10^6 \text{ km}^2$ (Curry and Moore, 1971; Curry et al., 1982; Emmel and Curry, 1984). Channels up to 2500 km long act as conduits for turbidity currents flowing the full length of the fan from its apex in the northern Indian Ocean off the Ganges Delta until it merges with the central abyssal plain south of the equator. The distal parts of this fan complex are spectacularly affected by deformation associated with the diffuse plate boundary zone across the northern Indian Ocean. The objectives of this paper are to characterise the channel termination zone of the Bengal Fan and to study the complex interplay between sedimentation and tectonics in this unique area.

It is now recognised that the zone of diffuse deformation in the northern Indian Ocean, representing the plate boundary between the Indian and Australian plates, extends for thousands of kilometres from the Chagos Bank to the Sumatran Trench (Gordon et al., 1990). Within the Central Indian Ocean Basin this deformation manifests itself tectonically with an E-W fabric on two spatial scales: long wavelength (150–200 km) undulations of basement and overlying sediments; and faulted blocks 5–20 km in width which are bounded by high-angle reverse faults that extend throughout the oceanic crust (Weissel et al., 1980; Bull, 1990; Bull and Scrutton, 1990; 1992).

The distal parts of the western Bengal Fan were the subject of a recent Ocean Drilling Program Leg (116) whose objectives were to investigate the timing and development of the deformation as well as the sedimentary history of the Bengal Fan. The principal results of the Leg (Shipboard Scientific Party, 1989) are briefly discussed here.

The first of the objectives was met by drilling a pair of companion sites on one of the fault blocks in the deformation area. One of these sites, 717, was in the thickest part of the axis of a syncline, whereas site 719 was partway up the block where syndeformational sediments are thinner. Sediments at both sites are fan turbidites with distinctive turbidite layers correlatable between the two sites. Reduction in thickness of the section between the two sites has occurred by pinching out of beds and thinning of individual turbidites. From the gradual nature of this reduction together with dating studies using calcareous nannofossils it was concluded that movement on the fault has been relatively slow and constant, perhaps with a slight increase with time. The onset of deformation was 7.5 - 8.0 Ma.

The second objective, the sedimentary history of the distal Bengal Fan, was met partly by sites 717 and 719 and partly by drilling on the next block south where the post-Miocene section is attenuated, thus allowing penetration of older sediments. At the base of this hole (site 718) fan sediments of early Miocene age (17 Ma) were still being penetrated with no evidence for reaching the base of the Fan. Almost the entire Miocene section consists of silt and silty mud turbidites.

The best studied area of the deformation zone is just to the south of the Leg 116 sites where there is now reasonable data coverage (see Figure 2, for example). Authors have looked in detail at the tectonic deformation in this area from seismic reflection profiles (Neprochnov et al., 1988; Bull, 1990; Bull and Scrutton, 1990; 1992). These studies have concentrated on the deeper structure of the deformation. In this paper we use 3.5 kHz profiles, in combination with 12 kHz echograms, seismic reflection profiles and core data, to study sedimentary processes and their interaction with the two spatial scales of deformation. The dataset used in this study was collected by Lamont-Doherty Geological Observatory and Edinburgh University.

SEAFLOOR BATHYMETRY

Seafloor bathymetry is constrained by regularly spaced ship tracks in the south of the area (Fig. 2). In the north, the ship tracks are clustered around the ODP drilling sites, so the bathymetry is only well constrained in this small region. Seafloor depths range from 4500m in the north of the study area to 5100m in the south, whilst just to the east the Afanasy-Nikitin Seamount rises some 2300m above the surrounding basin. If the effect of short wavelength bathymetric variations is ignored, the depth increases from north to south across the area by 600m over a distance of nearly 450km, as would be expected at the distal end of a sedimentary fan. The most prominent short wavelength feature is a seafloor high, centred at 80°00'E, 04°15'S, which rises about 400m above the surrounding seafloor. Its flanks slope at an angle of 0.6°. There is a smaller high, centred at 81°25'E, 04°45'S, which has a height of about 200m and flanks which slope at 0.8°.

It is observed that the seafloor bathymetry closely follows the basement topography, as determined by Bull (1990), with seafloor undulations, where present, orientated east-west and apparently discontinuous across north-south orientated fracture zones.

CHANNEL CHARACTERISTICS

In the surveyed area, 35 crossings of submarine channels have been identified from 3.5kHz and 12kHz echosounder and from seismic reflection sections (Fig. 3). The channels can be classified by their topographic relationship to the local mean surface of the fan. About 60% of the channels are incised below the local fan surface representing erosional or scoured features and the remaining 40% are built up above it representing depositional features (Normark, 1970). Channel depths range between 3 and 41m, with 65% of channels having depths less than 10m. As the angle of a ship's track across a channel is, in most cases, unknown, the channel widths calculated from echosounder profiles are unreliable. However, the maximum recorded apparent

width of 3500m places an upper limit on true channel widths. The minimum recorded width is 180m. Around the ODP sites, the high density of ship tracks allows two erosional channel paths to be traced across a small distance (approximately 10km). In this case, true widths of 750m and 1090m were calculated for the two channels. In general, the wide spacing of ship tracks relative to the presumed complexities of channel pathways (Damuth et al., 1983, Carter, 1988), over most of the area prohibits accurate channel path determination. However, several other channel characteristics have been noted. The channel lettering employed below refers to Figures 3 and 4.

Channel A is wide and shallow with levees which are only slightly raised. Over both levees, the echosounder profile shows a long acoustic return with a strong bottom echo and no sub-bottom reflections. The echo length decreases with increasing distance from the channel axis. In the channel itself, the acoustic return is shorter although the bottom echo is still strong, and the lack of acoustic penetration and sub-bottom reflections suggest that the channel is floored by sandy sediments whose surface is broken up by bedforms produced by turbidity currents (Damuth, 1975). Active depositional channels are typically floored by sandy sediments whose sand content decreases further away from the channel floor (Normark, 1978), and given the width and low relief of channel A, it is interpreted as an active depositional channel with levees which are just starting to develop.

Channel E is a good example of a more established depositional channel. Weak but coherent reflections are present in the levees and the channel itself and both levees are built up above the local mean surface of the fan.

In a small part of the area, centred at 80°50'E, 03°35'S, three large depositional channels appear on three different sections of the echosounder profile. Channel F is imaged by one of the sections. Some incoherent reflections are present in the levees and the channel floor comprises weak, prolonged echoes. One of the channel walls appears to have slumped down to the channel floor, producing an asymmetric profile. On the basis of their similar seismic character, their equivalent dimensions and close physical proximity, these three imaged channels are

almost certainly part of the same system, and this is by far the largest in the surveyed area with a depth of 41m. Therefore, it may be one of the main active distributary channels of the fan, in this area. The recorded positions of this channel indicate that it follows a meandering path, the wavelength of which appears to be 30km over this small section.

Channel B is bounded to the right by a 10m high fault block which comprises a strong seafloor echo with several continuous, parallel sub-bottoms, whereas weaker, prolonged echoes are returned from the channel floor itself. As the channel is flush with the base of the fault scarp, it seems likely that the channel path has been controlled by fault-induced bathymetry. Therefore, the faulting most likely occurred prior to the development of this part of the channel.

Within the surveyed area, there are several examples of channels which have been partly or completely infilled by younger sediments. In the case of channel C, the profile is visible as a weak sub-bottom reflection. The infilling sediments are acoustically transparent with a strong bottom echo. Damuth (1980a, 1980b) suggested that this type of echogram is typical of a mass-wasting process, such as a debris flow. However, as the channel is situated at the very distal end of the fan where regional slopes are minimal, the debris flow was probably a local event derived from a fault block high, or the channel has been filled by homogeneous fine-grained muds.

The scoured, erosional channels mentioned earlier are typified by channel D. The echoes over this channel are weak and prolonged with a strong bottom return, indicating limited acoustic penetration. The channel appears "V"-shaped because of the vertical exaggeration on the echosounder profile. It has no levees and a faint diffraction pattern extends down from the base of the channel. In the surveyed area, this type of channel is no more than 10m deep and usually has an apparent width of less than 1000m. Thus, scoured channels appear to be narrower than depositional channels, whereas channel depths are similar for both types.

Most of the channels, including the main distributary one centred at 80°50'E, 03°35'S, are located in the deeper, flatter parts of the area. However, a partially infilled channel can be seen located at a point about 100m below the summit of the main seafloor high already noted. In this channel, an acoustically transparent layer has been deposited which onlaps onto the

levees. The data quality along this section of 3.5kHz echosounder profile is very poor, but several other channels have been tentatively identified over the summit of the seafloor high. These indistinct channels are assumed to be inactive as it is unlikely that active channels would continue up the inclined side of the seafloor high. A probable explanation for their occurrence is that they developed prior to the uplift of the seafloor high which is coincident with the crest of a long wavelength basement undulation. This uplift rendered them inactive and allowed them to become subsequently infilled by more recent sediments, presumably hemipelagic or hemiturbidite.

Two almost totally infilled channels have been identified in the north of the survey area near the ODP sites (one of them being channel C, which has been described earlier). In both cases, the old channel profile remains visible as a sub-bottom reflection and the infilling material is acoustically transparent. There are, at least, two major faults in this region, both of which downthrow towards the south. It is possible that the faults have undergone displacement in both a lateral, as well as vertical sense which may have diverted the paths of existing channels in the area, thus rendering some channel sections inactive.

ECHO CHARACTER MAPPING

Echo character mapping has been completed in the surveyed area using 3.5kHz echosounder profiles. Five distinct echo types have been identified, and their nature and distribution throughout the area are shown in Figures 2 and 5. The echo type interpretation follows Damuth (1975, 1980a, 1980b).

Echo type 1 (Fig. 5) comprises a very prolonged echo with a strong seafloor return. No sub-bottom reflections are visible. This echo type appears to be the same as the class IIB echoes in the classification scheme developed by Damuth, which are associated with sediments comprising, on average, 54% silt/sand beds and 46% mud. It has been suggested that the prolonged echoes and lack of sub-bottoms, which characterize echo type 1, could be a result of scattering of acoustic energy either by erosional/depositional bedforms on the seafloor and/or by

relatively thick sand/silt beds (Damuth, 1975, 1978, 1980a, Damuth and Hayes, 1977, Embley, 1976). If the acoustic energy is scattered at the seafloor, then less energy is transmitted and the prolonged echo from scattering masks sub-bottom reflections. Damuth suggests that high velocity turbidity currents are responsible for producing the large amounts of silt/sand present in the sediments, and also for producing erosional/depositional bedforms. Thus, echo type 1 is interpreted as sediments of mainly turbiditic origin.

Echo type 2 (Fig. 5) comprises a prolonged echo with weak, widely spaced, coherent, parallel sub-bottom reflections. Although this echo type is not included in Damuth's classification scheme, it is most similar to the class IIB echoes; the differences being that echo type 2 has a slightly less prolonged echo with one or two sub-bottoms present. These differences are thought to indicate that there is less silt/sand present than in echo type 1 and also that acoustic energy is still being scattered at the seafloor, but to a lesser extent than in echo type 1, so the depth to which sub-bottoms are recorded increases. The reduction in seafloor scattering implies that there may be fewer erosional/depositional bedforms present and therefore, the sediments responsible for echo type 2 may have been deposited by weaker and/or more muddy turbidity currents than in the case of type 1 echoes.

Type 3 echoes (Fig. 5) comprise a slightly prolonged echo with indistinct, generally discontinuous sub-bottoms of varying lateral extent, and a clear seafloor reflection. This description fits the class IIA echoes in Damuth's classification scheme. The average bedded silt/sand content of sediments generating type 3 echoes was found to be 11% (Damuth, 1980a). The echo type is thought to be caused by the presence of erosional/depositional bedforms patchily distributed across the seafloor, which results in a differential scattering of acoustic energy and, therefore, semi-prolonged echoes with intermittent sub-bottoms are recorded.

Echo type 4 (Fig. 5) comprises multiple distinct, closely spaced, parallel sub-bottom reflections which are mostly laterally coherent, although they vary in reflectivity. There are hardly any prolonged echoes and the seafloor reflection is clear and continuous. This echo type falls into class IB of Damuth's classification scheme, and the associated sediments have an

average bedded silt/sand content of 3% (Damuth, 1980a). According to Damuth, echoes can be generated by interference from many thin layers and also be produced by factors such as changes in density and CaCO_3 content, and differential sediment compaction and grain size. Therefore, the sub-bottoms are not directly related to individual beds. The paucity of silt/sand beds suggests that sediments generating type 4 echoes are either less controlled by turbidity currents or, more likely, are entirely mud-rich turbidites. These are generally found in the more distal regions of the fan and adjacent to the main distributary channel pathways.

It can be seen from the previous descriptions that echo types 1 and 4 represent the end members of a continuous sequence. Progressing from type 1 to type 4, the echoes become less prolonged and sub-bottoms appear and become more closely-spaced and coherent. These echo variations correspond to a decrease in the bedded silt/sand content of the sediment and possibly to a reduction in the number of erosional/depositional bedforms present on the seafloor, amongst other factors. Thus, the sequence of echo types from 1 to 4, is interpreted to represent environments of deposition which are progressively more mud rich. Turbidity currents have progressively lost their silt/sand load and mud turbidites are more interbedded with thick hemipelagic and hemiturbidite deposits. They are generally more distal in setting.

Echo type 5 comprises a weak seafloor echo and is internally acoustically transparent. Along some parts of the echosounder profile, the acoustically transparent layer overlies sediments with a different echo character. Its thickness can be up to 20m but is usually less than 10m. The transparent layer occurs over a small region which is centred at $79^{\circ}30'E$, $04^{\circ}15'S$ and lies immediately west of the main seafloor high (Fig. 2). The transparent layer has been recorded in this region by both the Vema 2902 and Robert Conrad 2706 cruises.

Along two sections of RC2706 echosounder profile, both of which are orientated approximately north-south, the transparent layer has accumulated in the form of a drape deposit, up the north-facing slopes of fault blocks and small topographic highs only. This suggests that the acoustically transparent sediments were deposited from a southward travelling flow. However, preferentially accumulated transparent sediments are not seen on any other sections of

profile over the region, so it is possible that the southward flow was very weak, or that localized reworking of sediments by bottom currents is responsible for the observed accumulations.

It is suggested that echo type 5 could be generated by a series of hemiturbidite deposits, as described by Stow and Wetzel (1990). They define a hemiturbidite as a very fine-grained muddy sediment with no distinct bedding, partly turbiditic, partly hemipelagic in character that is deposited from an essentially stationary, dilute suspension cloud which is formed from, but beyond and above the dying stages of a large turbidity current. Hemiturbidites are most likely to occur in distal turbidite settings and can be deposited over a period of at least a few months for a unit 1m thick. Consequently they are bioturbated throughout most of their thickness and this bioturbation causes complete homogenisation of these very fine-grained sediments rendering them acoustically transparent internally.

Seismic p-wave velocities were found to be anisotropic at the base of some hemiturbidite beds (Stow and Wetzel, 1990) which indicates that the lowermost units of these beds were deposited from a very dilute turbidity current. The same dilute nature could explain the accumulations of acoustically transparent sediments up north-facing slopes that originated from generally southward directed flows, and also the acoustically transparent fills of some abandoned channels. However, the confinement of the sediment fill to the channel axes argues against a true hemiturbidite deposit in this case.

SEDIMENT CORES AND THEIR RELATIONSHIP TO ECHO CHARACTER

Within the surveyed area, the results from three Ocean Drilling Program sites and eleven piston cores taken by the Lamont-Doherty Geological Observatory were available. The sediments recovered from all fourteen sites are dominated by turbiditic inputs with only very minor pelagic intercalation.

The boreholes from the three closely spaced ODP sites (717, 718 and 719) drilled at approximately 81°24'E, 01°00'S, all show very comparable lithostratigraphic sections (Stow et al., 1990). These are dominated by turbidites from four main sources: thin to very thick-bedded silt/sand and mud turbidites derived from a Himalayan source; thin to thick dark mud turbidites

derived from the east Indian continental margin having a marked Deccan Traps signature; nannofossil mud turbidites from the south Indian and Sri Lankan margin; and pale foraminiferal-rich turbidites from a local seamount source. Pelagic intercalations are minimal but thick sections of hemiturbidite deposits occur in parts. This facies association extends to the base of each borehole drilled, i.e. to a depth below seafloor of 961m in the longest borehole.

The eleven piston cores have a length which ranges between 48cm and 964cm and has an average value of 472cm. The core sites are widely dispersed over the surveyed area and the recovered sediments can be broadly divided into three categories (see Table 1). One core in the north of the area (RC17130) comprises layers of foraminiferal marl, and interbedded terrigenous clay and foraminiferal marl. These sediments appear to be the product of alternating pelagic and turbiditic inputs.

The second category consists of cores with sandier sediments. Cores VM29037 and VM19173 are situated approximately in the middle of the area and comprise sediments with nearly 100% quartz sand content overlain by yellow/brown coloured clay, which is approximately 0.7m thick, with less than 1% sand content. Further to the south, core VM29038 comprises sediments with a slightly lower quartz sand content (between 70% and 95%), present throughout the core. Also in the south of the area, core VM19172 consists of interbedded silt and sand/silt zones which have sand contents of 30% and 85% respectively. Sediments generally have a lower coarse fraction as they are deposited progressively further away from their terrigenous source, with the exception of sediments from core RC17130, and this is consistent with the observed decrease in sand content from the centre of the area southwards. The main distributary channel identified in the area is located near to one of the cores with a high sand content.

The remainder of the piston cores consist of clays which have a sand content of between 0% and 3% and are rarely laminated. The clays contain varying proportions of radiolaria, volcanic glass shards, sponge spicules, mica and quartz. In two of these cores, VM36058 and VM36059 situated in the east of the area near the base of the Afanasy-Nikitin seamount, an

18cm thick layer of volcanic mud is present at the top of the cores which could be the result of a recent seamount eruption, possibly resedimented down the side of the seamount. However, the rest of the sediments in this category are mostly terrigenous turbidites, with predominant micaceous silts and muds that originated from the Himalayas and reached the Bengal Fan via the Ganges Delta (Curry and Moore, 1971, Stow and Cochran, 1989).

Out of the eleven piston cores, seven contained manganese micronodules, although there does not appear to be any pattern in the distribution of these cores over the surveyed area. The presence of micronodules is consistent with the findings of Bannerjee and Mukhopadhyay (1991) who observed that small (<4cm diameter) manganese nodules are most common north of 9°S, which would include this study area.

FAULTING

The recent faults in the survey area, which have been interpreted from 3.5kHz and 12kHz echosounder data, and seismic reflection profiles, fall into two categories. The majority of faults are expressed at the surface by rounded "hillocks" in the seafloor bathymetry (Fig. 6). In general, the base of one side of the hillock appears to be almost continuous with the surrounding seafloor, whereas, on the other side of the hillock, its base is delineated by a diffraction pattern which extends below the seafloor. Seismic reflection profiles (Fig 6, see Bull and Scrutton, 1992, for more discussion on their tectonic significance) show that these hillocks are, in fact, the hanging wall anticlines of the faults, with the diffraction pattern on the faulted side. In most cases, little or no structure can be seen in the hanging wall anticlines on echosounder profiles, but some display several small, closely spaced faults over their surface.

The major faults, which produce the hanging wall anticlines, have been seen on seismic reflection profiles to extend throughout the sedimentary cover and down into the oceanic crust (Bull and Scrutton, 1990, 1992). Echosounder profiles show that echoes from over the anticlines are usually weaker and shorter than echoes from the surrounding seafloor. This is possibly a result of slightly finer sediments being deposited post-faulting on these relative highs.

Some faults only appear as an offset in seafloor depth on echosounder records, but coincident reflection profiles demonstrate that they are real and also extend down to the basement. Basement faults which have not propagated upwards through the overlying sediment are imaged only by seismic reflection profiles and therefore, in areas surveyed by echosounder only, undetected basement faults are certainly present.

The maximum displacement of seafloor on either side of the fault, or fault block, is found to be 130m in this area, with an average of about 30m. The widths of the fault blocks range between 1km and 16km with an average of about 4km, and the fault blocks are tilted up to 5° above horizontal, the average value being almost 2°. The downthrow side of each fault is taken to be the side on which the seafloor is deepest. Within the survey area, 65% of all faults were found to downthrow towards the south, with the remainder downthrowing in a northerly direction. Bull (1990) found, on the basis of a seismic reflection profile study, that approximately equal numbers of faults downthrow south as downthrow north in this area. The discrepancy in these observations may be a product of the increased echosounder coverage in this study affording a more representative sample of the faults. Alternatively, it may indicate that faults downthrowing to the south have propagated further through the sedimentary cover and are therefore the most recently active and are the ones recognised preferentially on high-resolution (3.5kHz) profiles.

The level of recent activity of the faults has been roughly assessed following the criteria that the more recent faults are sharply defined on the echosounder profiles, with little or no erosion over the fault block surface and no build up of sediments against the sides of the fault block. Three regions in which there are high numbers of active faults have been identified at 81°30'E, 02°50'S, 80°00'E, 04°15'S and 81°25'E, 04°45'S (see Figure 3). The latter two regions are situated on the two seafloor highs described earlier, which correlate with basement highs. The other region is situated on the south facing flank of an east-west trending undulation in the seafloor.

The number of faults, both active and inactive, is markedly higher over these three

regions and in general, there is a correlation between higher fault densities and the shallower parts of the survey area. Although this correlation is observed over the peaks of the east-west trending seafloor undulations in the west of the area, to some extent it may be a result of recent sediment infilling the troughs of the undulations, and therefore obscuring some of the faulting within these troughs. This is shown to be the case by seismic reflection profiles, on which basement faults are imaged within the troughs. These faults have not affected overlying sediments and are not seen on echosounder records. However, overall the correlation between fault activity and seafloor/basement highs is believed to be real.

DISCUSSION

Although the region surveyed in detail in this study is like a postage-stamp area at the end of the world's largest submarine fan, it nevertheless covers an area of 150-200,000 km². This is larger than most known modern fans and certainly far larger than almost all ancient turbidite successions that have been interpreted as submarine fans (Bouma et al., 1985a). It is important to bear in mind these scaling factors when considering the implications of this research to our understanding of fans in general (Bouma et al., 1985b). There are two aspects we wish to discuss further: (1) the nature of a channel-termination zone on a large mud-rich, elongate fan, and (2) the influence of within fan neotectonics on sedimentation.

Channel termination zone

According to previous work (Emmel and Curray, 1984; Stow and Cochran, 1989), the study area was beyond the reach of active channels at the feather edge of the fan where it merges with the Central Indian Ocean abyssal plain, over 2500km from its apex in the north off the Ganges delta. However, this work has shown that the fan channel system extends further south than previously recognised and that the region studied is, in fact, one broad zone of channel

termination.

The chief characteristics of this zone are illustrated in Figure 7 and include the following:

(a) There is a very low average down-fan gradient ($<1\text{m/km}$), with a locally irregular topography related to channel margins and structural highs (see below).

(b) There are a large number of low-relief channels, mostly $<10\text{m}$ deep but ranging up to 40m in depth, with widths varying from $<200\text{m}$ to $>1500\text{m}$. A great variety of channel types is evident, including broad flat-bottomed, narrow V-shaped, sediment-filled or unfilled, erosional and/or constructional. There is a marked lack of direct continuity of channels from one survey crossing to another that suggests meandering, bifurcation and terminations are common.

(c) Channel levees built up above the surrounding fan surface, by between 2m and 25m , are found flanking just less than half the channels surveyed and are typically a few km in width. In all cases levee heights are equivalent on left and right banks, attesting to the absence of a strong Coriolis force influencing deposition at these equatorial latitudes.

(d) The echocharacter distribution is complex. Four of the echocharacter types fall into the classification scheme developed by Damuth (1980a) and are readily interpreted in terms of turbidite deposition, ranging from more sand/silt-rich and higher energy currents (Type 1) to more mud-rich and lower energy currents (Type 4). There is a general north-south trend from Types 1-2 to Types 3-4, and also a topographic control with Types 1-2 occupying the lower ground. Both of these observations are consistent with a decrease in the influence and/or competence of turbidity currents across the channel termination zone, and with the fact that turbidity currents preferentially flow along bathymetric lows. Type 5 echoes are discussed

below.

(e) The sediments recovered from the three ODP sites in the north of the area and from the scattered piston cores to the south are dominantly turbiditic (Stow et al., 1990), including thin to very thick-bedded silt/sand and mud turbidites as well as nannofossil-foraminiferal bioclastic turbidites. Hemiturbidites were common in parts of the ODP boreholes (Stow and Wetzel, 1990) but pelagic sediments extremely rare. Turbidites from at least three distinct sources have been recognised at the ODP sites, showing that whatever is fed in the upper reaches of the fan system finds its way through to the channel termination zone.

Although the data are sparse regionally, there is a general southward decrease in sand/silt content observed in the cores that is consistent with the downfan change in echocharacter noted previously.

All the features noted above (a-e) might be considered as typical of a channel termination zone from any submarine fan, and particularly those of large, muddy elongate fans (Stow, 1981; 1986). Similar characteristics have been described from the Mississippi (O'Connell et al., 1991), Amazon (Damuth et al., 1983), Indus (Kolla and Coumes, 1987) and Laurentian (Piper et al., 1983) fans, as well as from a number of smaller fan systems (Normark, 1978; Bouma et al., 1985a; Droz and Bellaiche, 1985). The chief characteristic is one of complexity, in morphology, echocharacter and sediments, but with an organisation that is logical both spatially and temporally. Channel termination on smaller (radial) fans is most commonly in the middle fan region and is characterised by rapid dumping of sand-rich sediments, whereas on larger (elongate) fans the zone is more extended and the sediments finer grained.

However, there are several characteristics of the study area that we believe demonstrate the influence of within-fan neotectonic control on the otherwise normal pattern of deposition in a

channel termination zone.

Neotectonics and sedimentation

The distal parts of the Bengal fan lie within a broad area of active intraplate deformation that involves both the oceanic crust and overlying sediments (Bull and Scrutton, 1990, 1992). This has resulted in the otherwise 'smooth' low-gradient fan surface being interrupted by a series of rounded hillocks that are the surface expression of recent faulting. These create a local relief of typically 100-300m with gradients up to 5° above the horizontal. The interaction of this irregular topography with incoming turbidity currents results in several unique effects.

(a) Channels are diverted around the base of upstanding hillocks, and this may help contribute to channel meandering, switching and abandonment, although such processes also occur under normal conditions (eg. Kolla and Coumes, 1987). Channel remnants are left abandoned and now filled or partially filled on the flanks and crests of the hillocks, most likely as the direct result of tectonic uplift. The relative abundance of small erosional channels may be the result of local increase in flow velocities due to flow confinement around and/or over some of the hillocks.

(b) The complete lack of any detectable lobes in the whole of this channel termination zone is unusual for such a setting (eg. Normark et al., 1983) and we suggest that this results from topographic interference to incoming flows. Deposition is concentrated in the low-lying areas and is more ponded than lobate, with individual turbidites thinning up onto and pinching out against adjacent hillocks.

(c) The thinning and pinching out of turbidites over highs has been carefully documented in the region of the ODP sites (Stow et al., 1990), as also has the occurrence of hemiturbidites (Stow and Wetzel, 1990). Although flow lofting and upward mixing of fine-grained sediment into the

overlying water column is most likely a normal process for far-travelled turbidity currents (Sparks et al., 1993), the distal Bengal fan is the first area from which the resulting hemiturbidite deposits have been described. We suggest that the presence of irregular hillocks in this area serves to enhance the flow lofting process.

Echotype 5 is interpreted as reflecting an accumulation of hemiturbidites that have been deposited on the western flank of the main seafloor high as a result of flow lofting from southerly flowing westward diverted dilute turbidity currents. This inference remains circumstantial until corroborated by further coring in the area.

(d) There seems to be an abundance of small-scale slumping in the area as evidenced by chaotic reflectors associated with the margins of channels and with the more prominent hillocks. This local mass movement will be enhanced both by the presence of marked relief and by seismic activity related to fault displacement.

Although none of these features (a-d) are exclusive to zones of within-fan neotectonics, their relative abundance and co-occurrence are believed to be significant. The added influence of local relief and seismic activity to a channel termination zone will make an already highly varied depositional system still more complex in nature.

REFERENCES

- Bannerjee, R. and Mukhopadhyay, R., 1991. Nature and distribution of manganese nodules from three sediment domains of the Central Indian Basin, Indian Ocean. *Geo Marine Letters*, 11: 39-43.
- Bouma, A.H., Normark, W.R., and Barnes, N.E., 1985a. Submarine Fans and related turbiditic systems. Springer-Verlag. N.Y. 351pp.

- Bouma, A.H., Normark, W.R. and Barnes, N.E., 1985b. COMFAN: Needs and Initial Results. In: *Submarine Fans and related turbiditic systems*. Springer-Verlag. pp 7-12.
- Bull, J.M., 1990. Structural style of intra-plate deformation, Central Indian Ocean Basin: evidence for the role of fracture zones. *Tectonophysics*, 184: 213-228.
- Bull, J.M. and Scrutton, R.A., 1990. Fault reactivation in the Central Indian Ocean and the rheology of oceanic lithosphere. *Nature*, 344: 855-858.
- Bull, J.M. and Scrutton, R.A., 1992. Seismic reflection images of intraplate deformation, Central Indian Ocean basin, and their tectonic significance. *J. Geol. Soc. Lond.*, 149: 955-966.
- Carter, R.M., 1988. The nature and evolution of deep-sea channel systems. *Basin Res.*, 1: 41-54.
- Curry, J.R. and Moore, D.G., 1971. Growth of the Bengal deep-sea fan and denudation in the Himalayas. *Geol. Soc. Am. Bull.*, 82: 563-572.
- Curry, J.R., Emmel, F.J., Moore, D.G. and Raitt, R.W., 1982. Structure, tectonics and geological history of the North Eastern Indian Ocean. In: A.E.M. Nairn and F.G. Stehli (Editors), *The Ocean Basins and Margins*, Vol. 6. The Indian Ocean. Plenum Press, New York, N.Y.: 399-450.
- Damuth, J.E., 1975. Echo character of the Western equatorial Atlantic floor and its relationship to the dispersal and distribution of terrigenous sediments. *Mar. Geol.*, 18: 17-45.
- Damuth, J.E., 1978. Echo character of the Norwegian-Greenland sea: relationship to Quaternary sedimentation. *Mar. Geol.*, 28: 1-36.
- Damuth, J.E., 1980a. Use of high frequency (3.5-12 kHz) echograms in the study of near-bottom sedimentation processes in the deep-sea: a review. *Mar. Geol.*, 38:51-75.
- Damuth, J.E., 1980b. Quaternary sedimentation processes in the South China Basin as revealed by echo character mapping and piston-core studies. In: D.E. Hayes (Editor), *The Tectonic/Geologic Evolution of Southeast Asian Seas and Islands*. Am. Geophys. Union Monogr., 23: 105-125.
- Damuth, J.E. and Hayes, D.E., 1977. Echo character of the East Brazilian continental margin

and its relationship to sedimentary processes. *Mar. Geol.*, 24: 73-95.

Damuth, J.E., Kolla, V., Flood, R.D., Kowsmann, R.O., Monteiro, M.C., Gorini, M.A., Palma, J.J.C. and Belderson, R.H., 1983. Distributary channel meandering and bifurcation patterns on the Amazon deep-sea fan as revealed by long-range side-scan sonar (GLORIA). *Geology*, 11: 94-98.

Droz, L. and Bellaiche, G., 1985. Rhone deep-sea fan: morphostructure and growth pattern. *Am. Assoc. Petrol. Geol. Bull.*, 69: 460-479.

Embley, R.W., 1976. New evidence for the occurrence of debris-flow deposits in the deep sea. *Deep-Sea Res.*, 17: 267-270.

Emmel, F.J. and Curray, J.R., 1984. The Bengal submarine fan, Northeastern Indian Ocean. *Geo-Marine Letters*, 3: 119-124.

Gordon, R.G., DeMets, L. and Argus, D.F., 1990. Present day motion between the Australian and Indian plates: kinematic constraints on distributed lithospheric deformation in the Equatorial Indian Ocean. *Tectonics*, 9: 409-423.

Kolla, V. and Coumes, F., 1987. Morphology, internal structure, seismic stratigraphy and sedimentation of Indus fan. *Am. Assoc. Petrol. Geol. Bull.*, 71: 650-677.

Kolla, V., Moore, D.G. and Curray, J.R., 1976a. Recent bottom-current activity in the deep Western Bay of Bengal. *Mar. Geol.*, 21: 255-270.

Kolla, V., Sullivan, L., Streeter, S.S. and Langseth, M.G., 1976b. Spreading of Antarctic Bottom Water and its effects on the floor of the Indian Ocean inferred from bottom-water potential temperature, turbidity and sea-floor photography. *Mar. Geol.*, 21: 121-189.

Neprochnov, Y.P., Levchenko, O.V., Merklin, L.R. and Sedov, V.V., 1988. The structure and tectonics of the intraplate deformation are in the Indian Ocean. *Tectonophysics*, 156: 89-106.

Normark, W.R., 1970. Growth patterns of deep-sea fans. *Am. Assoc. Petrol. Geol. Bull.*, 54: 2170-2195.

Normark, W.R., 1978. Fan valleys, channels and depositional lobes on modern submarine fans: characters for recognition of sandy turbidite environments. *Am. Assoc. Petrol. Geol. Bull.*, 62:

912-931.

Normark, W.R., Gutmacher, C.E., Chase, T.E. and Wike, P., 1983. Monterey Fan: Growth pattern control by basin morphology and changing sealevels. *Geomarine Letts.* 3: 93-100.

Piper, D.J.W., Normark, W.R. and Stow, D.A.V., 1983. The Laurentian Fan - Sohm Abyssal Plain. *Geo-Marine Letts.* 3: 141-146.

O'Connell, S., Ryan, W.B.F and Normark, W.R., 1991. Evolution of a fan channel on the surface of the outer Mississippi Fan: evidence from side-looking sonar. In: *Seismic Facies and Sedimentary Processes of Submarine Fans and Turbidite Systems.* Springer-Verlag, NY.

Sclater, J.G. and Fisher, R.L., 1974. Evolution of the east Central Indian Ocean, with emphasis on the tectonic setting of the Ninetyeast Ridge. *Geol. Soc. Am. Bull.*, 85: 683-702.

Shipboard Scientific Party, 1989. ODP Leg 116 site survey. In Cochran, J.R., Stow, D.A.V., et al., 1990. *Proc. ODP, Init. Repts.*, 116: College Station, Tx (Ocean Drilling Program), 197-210.

Sparks, R.S.J., Bonnetaze, R.T., Huppert, H.E., Lister, J.R., Hallworth, M.A., Mader, H., and Phillips, J., 1993. Sediment-laden gravity currents with reversing buoyancy. *Earth Planet. Sci. Lett.*, 114: 243-257.

Stow, D.A.V., 1981. Laurentian Fan: morphology, sediments, processes and growth pattern. *Am. Assoc. Petrol. Geol. Bull.*, 65: 375-393.

Stow, D.A.V., 1986. Deep Clastic Seas. In: Reading, H.G., ed., *Sedimentary Environments and Facies*, 2nd edition, Blackwells, Oxford, pp 399-444.

Stow, D.A.V, Cochran, J.R. and ODP Leg 116 Shipboard Scientific Party, 1989. The Bengal fan: some preliminary results from ODP drilling. *Geo-Marine Letters*, 9: 1-10.

Stow, D.A.V. and Wetzel, A., 1990. Hemiturbidite: a new type of deep water sediment. In: Cochran, J.R., Stow, D.A.V. et al., *Proc. ODP, Sci. Results*, 116: College Station, Tx (Ocean Drilling Program), 25-34.

Stow, D.A.V., Amano, K., Balson, P.S., Brass, G.W., Corrigan, J., Raman, C.V., Tiercelin, J-J, Townsend, M. and Wijayananda, N.P., 1990. Sediment Facies and Process on the Distal Bengal Fan, Leg 116. In: Cochran, J.R., Stow, D.A.V. et al., 1990. *Proc. ODP, Sci. Repts.*, 116:

College Station, Tx (Ocean Drilling Program), 377-396.

Weissel, J.K., Anderson, R.N. and Geller, C.A., 1980. Deformation of the Indo-Australian plate. *Nature*, 287: 284-291.

TABLE 1. PISTON CORE INFORMATION.

| PISTON CORE | LOCATION | DESCRIPTION |
|----------------|---------------------|--|
| RC17130 | 80°09'E, 00°56'S | Foraminiferal marl with some interbedded clay |
| VM19172 | 80°30'E, 05°32'S | Interbedded silt and sand with manganese nodules |
| VM19173 | 80°35'E, 03°15'S | Grey quartz sand |
| VM29010 | 80°52'E, 01°19'S | Green/grey fine-grained clay with manganese nodules |
| VM29037 | 79°11'E, 03°00'S | Grey clay overlying dark grey sand |
| VM29038 | 78°39'E, 05°43'S | Green/grey sand with manganese nodules |
| VM33055 | 81°42'E, 04°44'S | Grey/brown radiolarian clay |
| VM33057 | 81°41'E, 01°30'S | Yellow/grey clay, laminated in places |
| VM36057 | 81°38'E, 02°34'S | Yellow/brown clay with manganese nodules |
| VM36058 | 81°37'E, 02°31'S | Brown clay with manganese nodules and volcanic mud |
| VM36059 | 81°37'E, 02°29'S | Brown clay with manganese nodules and volcanic mud |

ACKNOWLEDGEMENTS

The authors are grateful to Jeff Weissel and Randy Lotti at Lamont-Doherty Geological

Observatory for providing access to 3.5kHz records and core data. The comments of two anonymous reviewers helped to greatly improve the manuscript. Edinburgh University data was collected during Charles Darwin cruise 28 and funded by NERC grant GR3/6480. LJR and this study were supported by NERC grant GR9/441.

FIGURE CAPTIONS

Figure 1. Location map showing position of survey area and ODP Leg 116 sites in the Central Indian Ocean. Bathymetry in metres. (After Emmel and Curray, 1984)

Figure 2. Map of bathymetry of survey area, and echo character of seafloor showing the distribution of the various echo types described in the text and shown in Figure 5. Location of 3.5kHz echograms (ship tracks) are shown.

Figure 3. Map showing positions of channel crossings on echosounder profiles, and areas of active faulting. The lettered channels are described in the text and shown in Figure 4. Note that areas of active faults correlate with seafloor highs.

Figure 4. Diagram showing channel profiles recorded by 3.5kHz echosounder with associated line drawings. A: active depositional channel, B: erosional channel bounded to the right by a fault block, C: infilled channel, D: typical erosional or scoured channel, E: typical depositional channel, F: large depositional channel, thought to be one of the main distributary channels in survey area.

Figure 5. Diagram showing examples of the five echo types recorded by 3.5kHz echosounder in the survey area, and described in the text. Type 1: very prolonged echo with a strong seafloor return and no sub-bottom reflections, type 2: prolonged echo with widely-spaced, coherent, parallel sub-bottom reflections, type 3: slightly prolonged echo with indistinct, discontinuous sub-bottom reflections, type 4: multiple distinct, closely-spaced, parallel sub-bottom reflections, type 5: acoustically transparent layer with weak seafloor echo. See text for further discussion.

Figure 6. One of the spectacular reverse faults within the intraplate deformation zone (at 81°27'E, 02°29'S) as revealed on A) 3.5kHz echosounder record, and B) a migrated multichannel (12-fold) seismic reflection profile. The fault plane has a dip of 35-40° within oceanic basement (the top of which is denoted by the strong reflector at c. 7.4 seconds TWT). The dip steepens above basement and there are a complex set of faults within the sedimentary cover. The 3.5 kHz record shows evidence of large-scale slumping. See Bull and Scrutton (1990, 1992) for more discussion of the seismic reflection profiles.

Figure 7. Schematic diagram of the Channel Termination Zone showing inferred channel pathways (based on actual channel crossings and echo character mapping), areas of positive relief related to tectonic activity, the Afanasy Nikitin Seamount, and the nature of sedimentation resulting from interaction between current input and tectonic relief. Bathymetry of the Afanasy Nikitin Seamount adapted from Sclater and Fisher (1974) using CD28 bathymetric data.

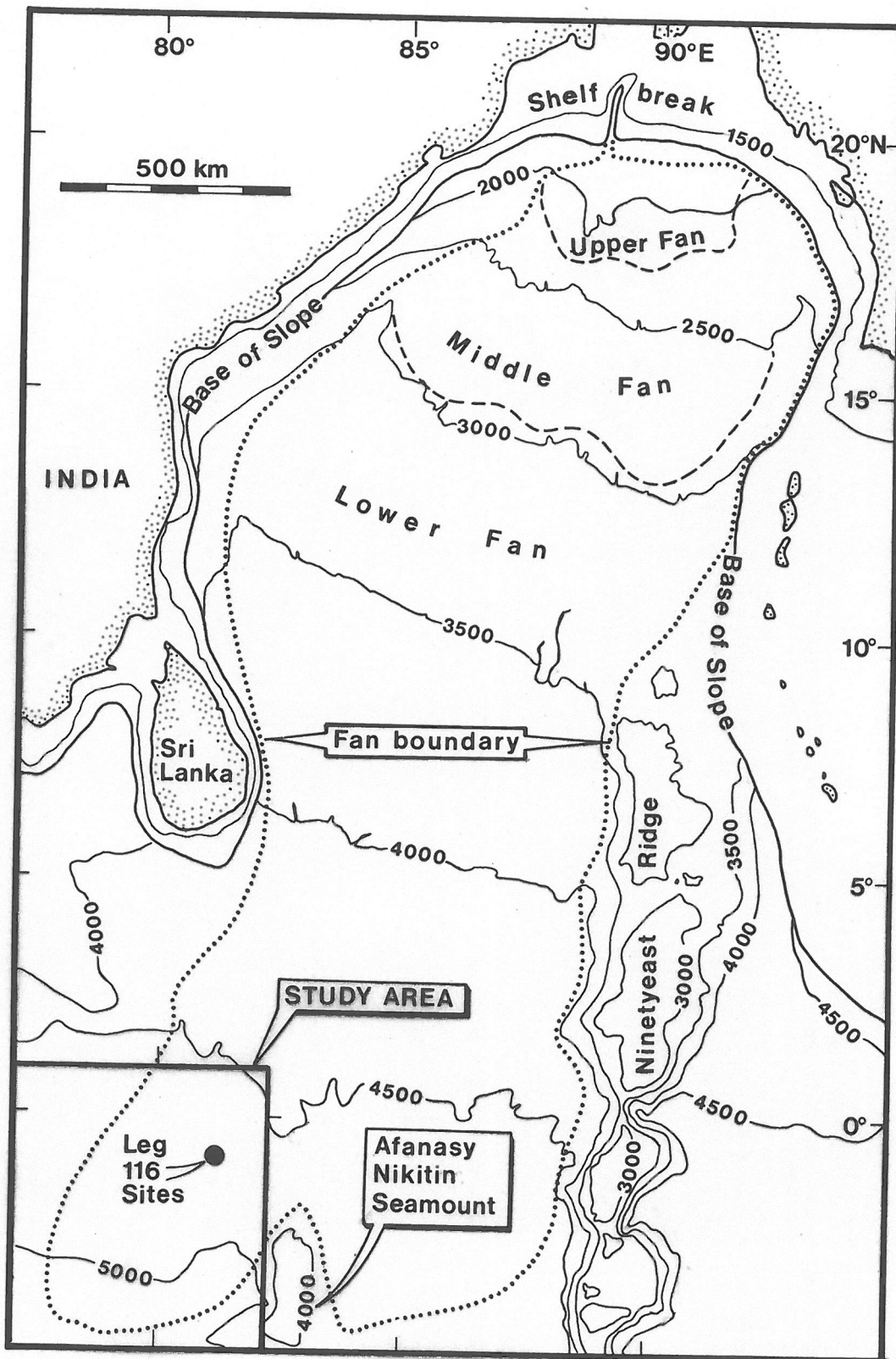


Fig 1

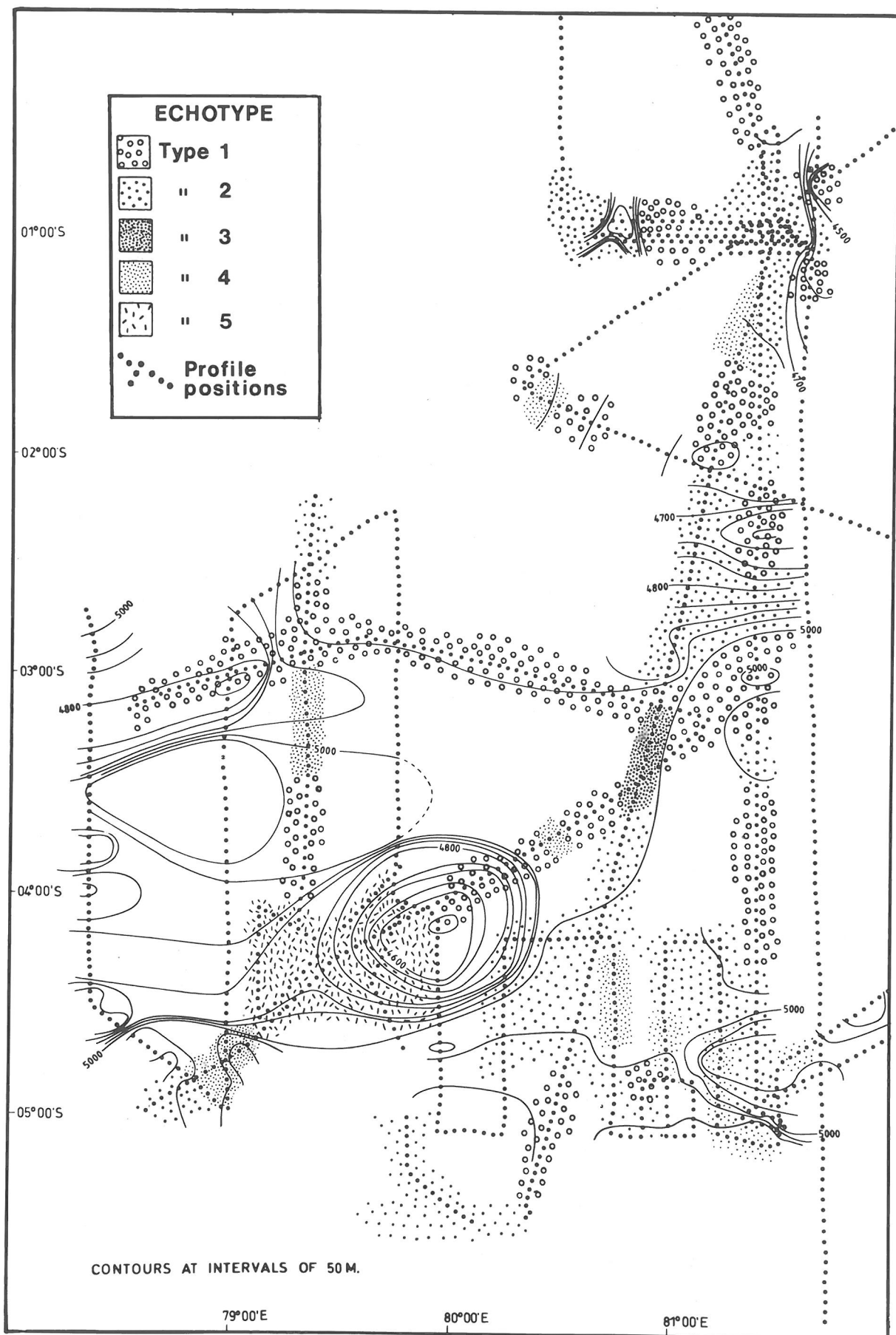


Figure 2.

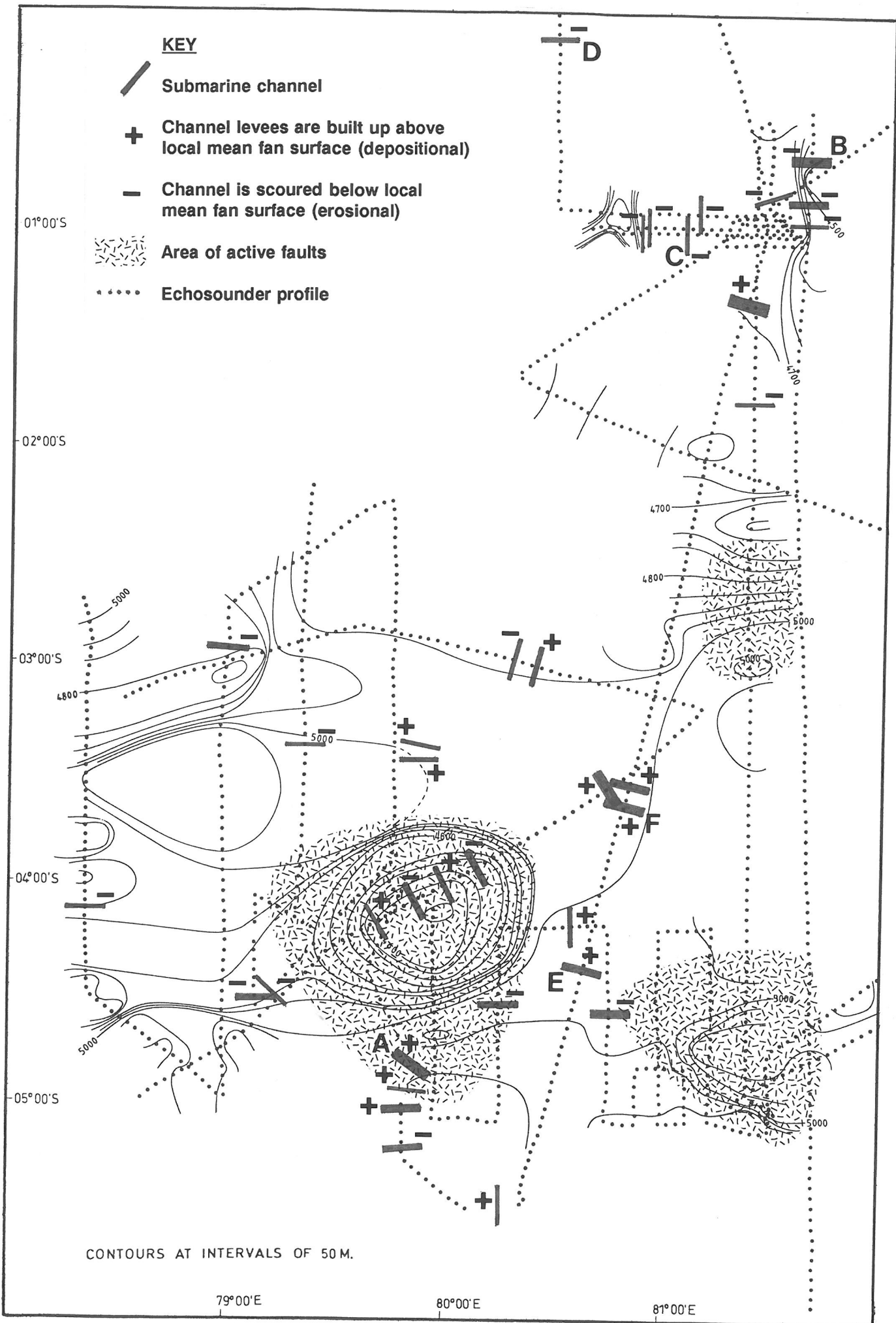


Figure 3.

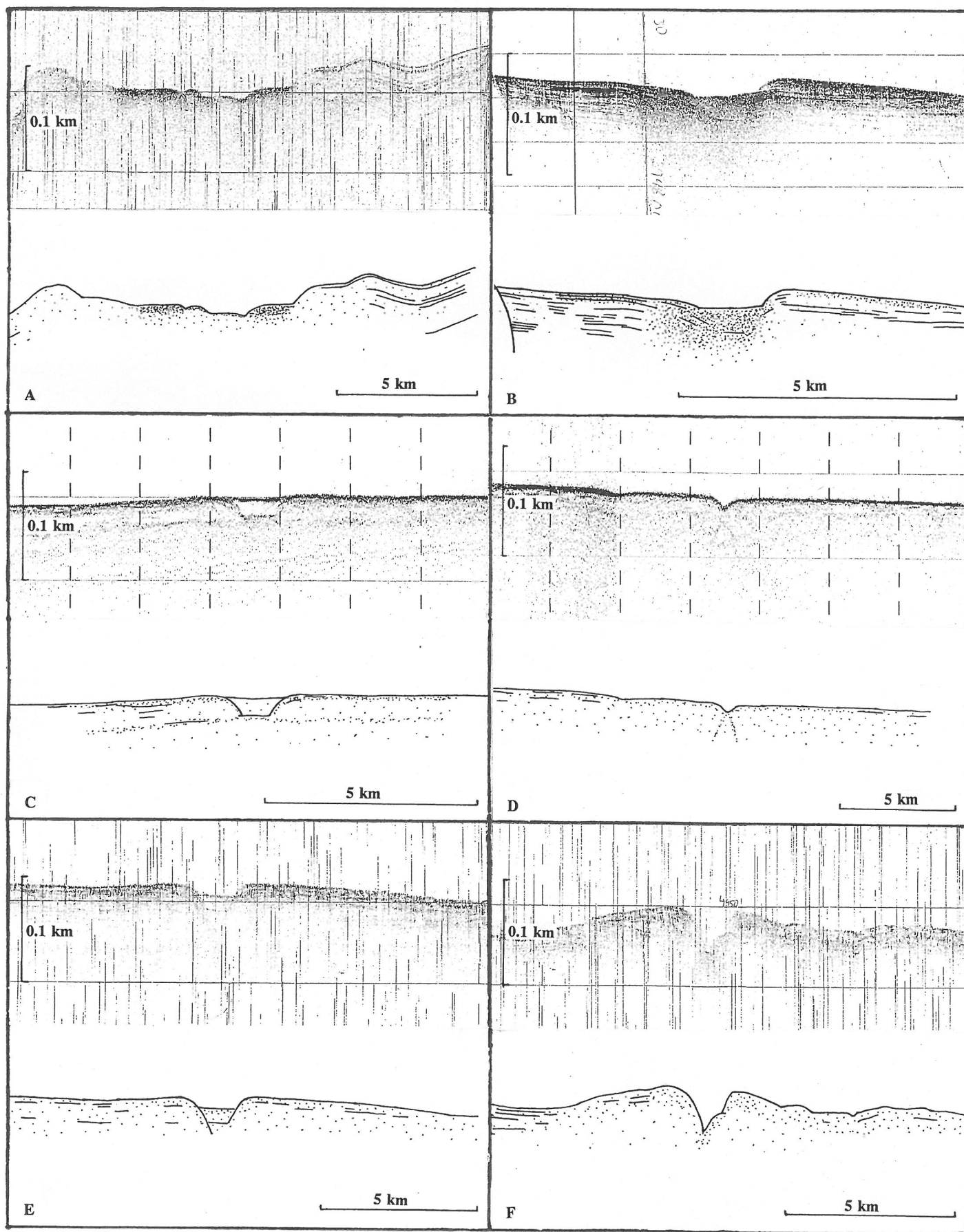


Figure 4.

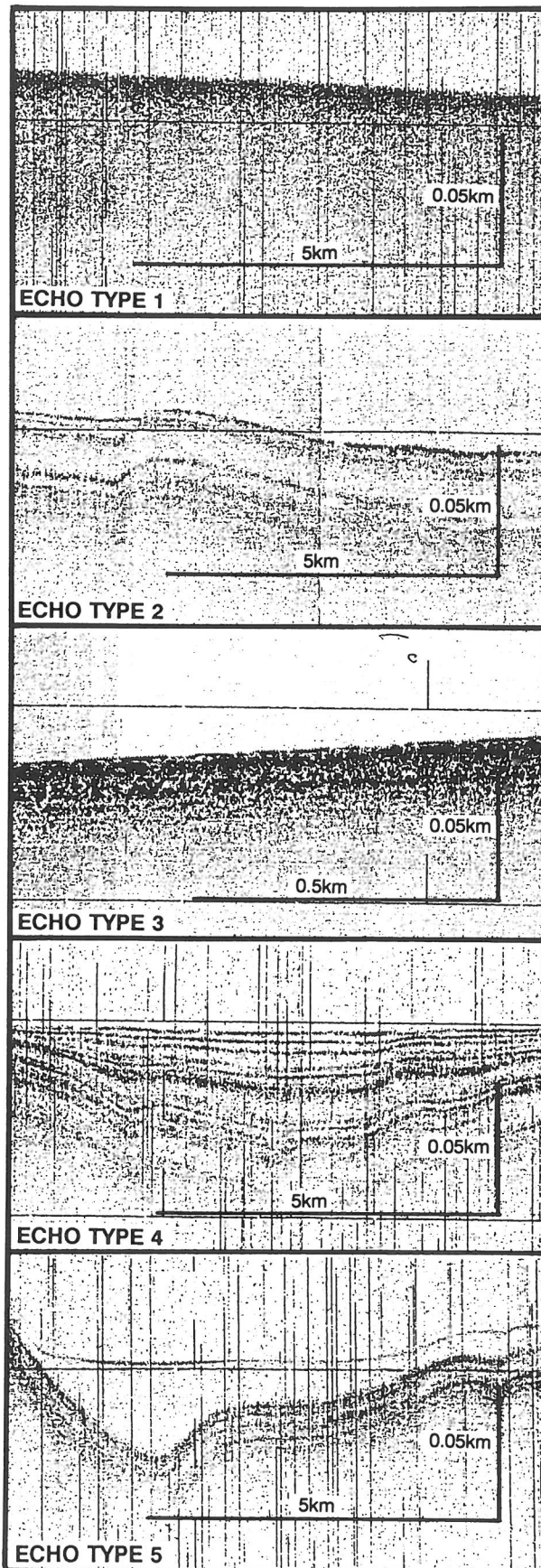


Figure 5.

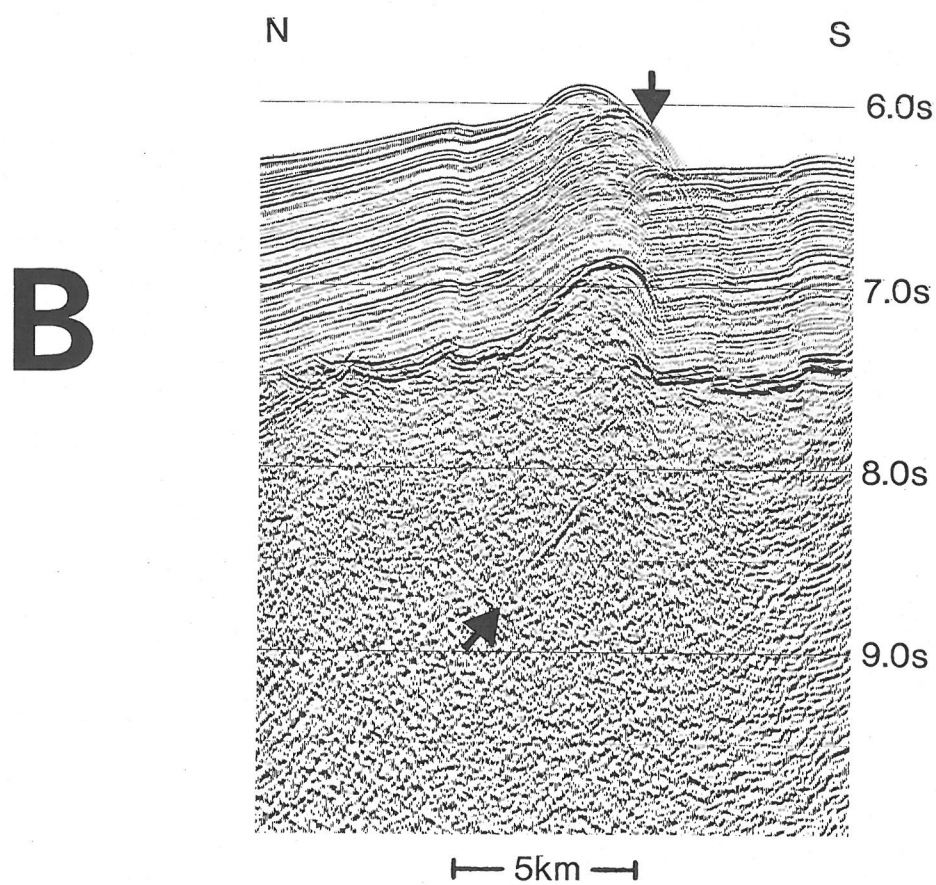
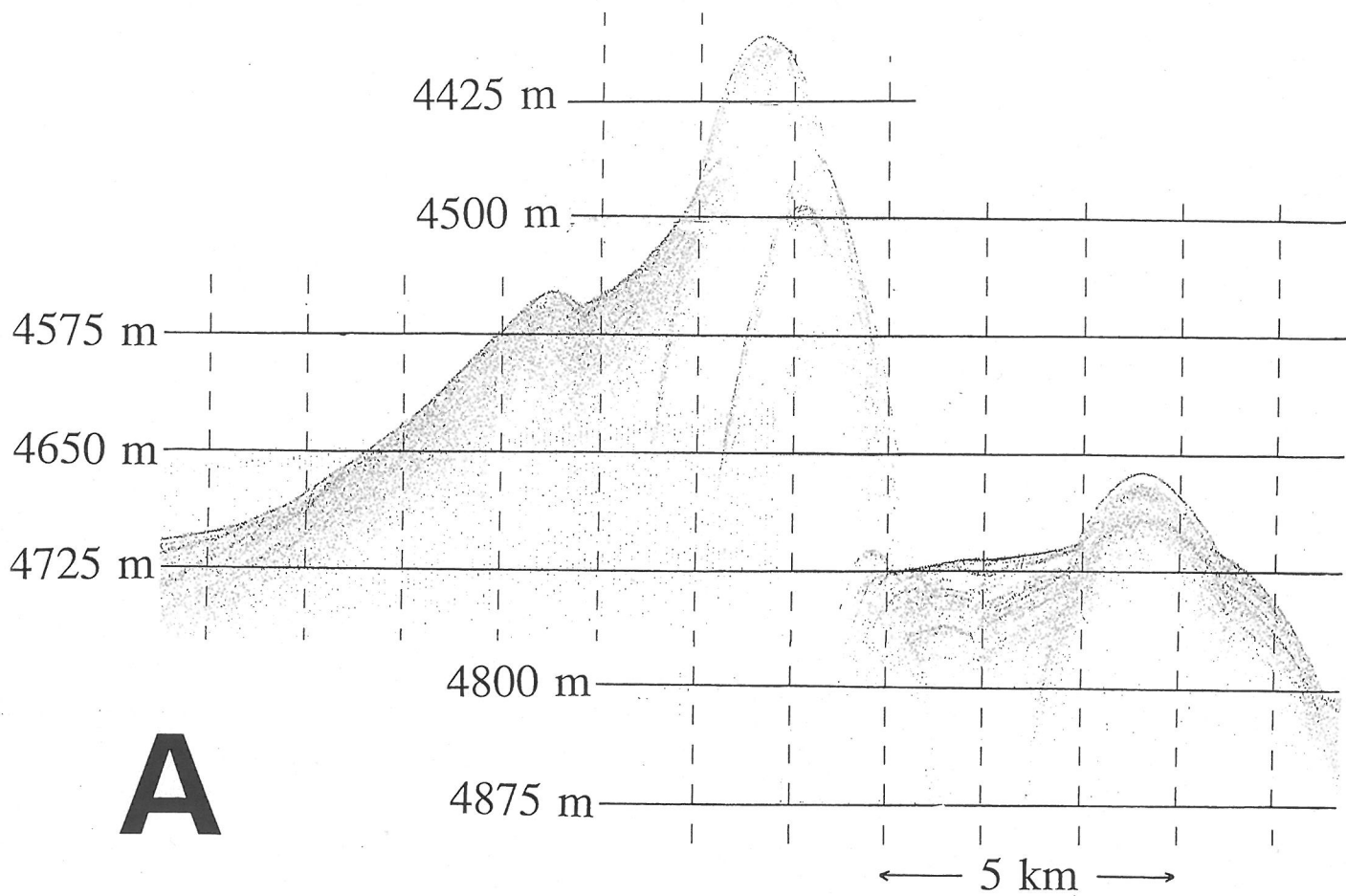


Fig. 6.

